

Extended Barbaralanes: Sigmatropic Shiftamers or σ -Polyacenes?

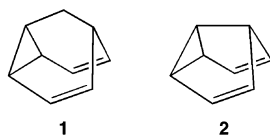
Dean J. Tantillo,^{*,†,‡} Roald Hoffmann,[†] Kendall N. Houk,[§] Philip M. Warner,[⊥]
Eric C. Brown,^{||} and Daven K. Henze^{||}

Contribution from the Department of Chemistry and Chemical Biology, Cornell University, Ithaca, New York 14853-1301, Department of Chemistry and Biochemistry, University of California, Los Angeles, California 90095-1569, Department of Chemistry and Chemical Biology, Northeastern University, Boston, Massachusetts 02115, and Department of Chemistry, University of Washington, Seattle, Washington 98195

Received October 25, 2003; E-mail: tantillo@chem.ucdavis.edu

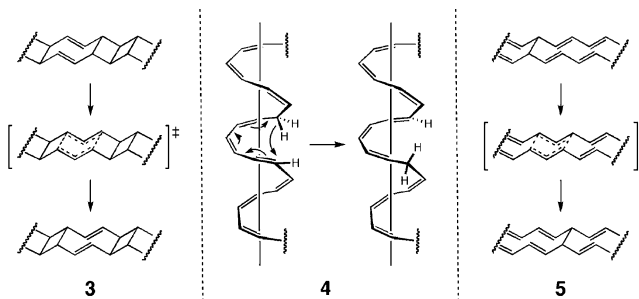
Abstract: Starting from fused barbaralanes, we come (theoretically) to a new class of delocalized molecules in which two polyenyl radical chains interact with each other through space in a bonding way, but do not form full σ -bonds. These molecules resemble σ -homologues of polyacenes and are bishomoaromatic.

The study of Cope rearrangements¹ in rigid polycyclic systems such as barbaralane (**1**)^{2,3} and semibullvalene (**2**)^{3,4} has a long history, crafted by some of the foremost physical organic chemists of the past half-century. The geometric restrictions of these polycyclic frameworks—often modulated by the electronic effects of attached substituents—have been used to lower the barrier for Cope rearrangement, in some cases to the point where a delocalized, C_{2v} -symmetric structure actually becomes a minimum rather than a transition structure for [3,3]-sigmatropic rearrangement. Such structures are 6π electron neutral bishomoaromatic species.^{2c}

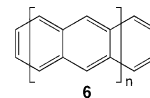


Recently, we described (on paper) several examples of a new class of molecules called sigmatropic shiftamers:⁵ polymers with localized substructures that propagate along the extended chain via sigmatropic rearrangements (for example, **3** and **4**, Scheme

Scheme 1



1). The first type of shiftamer reported (**3**) involved the movement of a pair of parallel π -bonds along a ladderane polymer via [3,3]-sigmatropic shifts.^{5a} We initially also proposed σ -bond movement along a pair of parallel polyene chains via [3,3]-sigmatropic shifts (**5**).^{5a} We now report that systems based on **5** seem unwilling to behave as shiftamers, but rather behave as analogues of polyacenes (**6**). The molecules we will discuss include the first examples, predicted computationally, of 10π , 14π , and 18π bishomoaromatic species.



[†] Cornell University.

[‡] Current address: Department of Chemistry, University of California, Davis, One Shields Avenue, Davis, CA 95616.

[§] University of California.

[⊥] Northeastern University.

^{||} University of Washington.

- (1) For leading references, see: (a) Gajewski, J. J. *Hydrocarbon Thermal Isomerizations*; Academic: New York, 1981. (b) Goldstein, M. J.; Benzon, M. S. *J. Am. Chem. Soc.* **1972**, *94*, 7147–7149. (c) Wiest, O.; Montiel, D. C.; Houk, K. N. *J. Phys. Chem. A* **1997**, *101*, 8378–8388. (d) For a recent study from one of our groups on Cope rearrangements in geometrically constrained systems, see: Tantillo, D. J.; Hoffmann, R. *J. Org. Chem.* **2002**, *67*, 1419–1426.
- (2) For leading references, see: (a) Quast, H.; Seefelder, M.; Becker, C.; Heubes, M.; Peters, E.-M.; Peters, K. *Eur. J. Org. Chem.* **1999**, 2763–2779. (b) Doering, W. v. E.; Ferrier, B. M.; Fossel, E. T.; Hartenstein, J. H.; Jones, M., Jr.; Klumpp, G.; Rubin, R. M.; Saunders, M. *Tetrahedron* **1967**, *23*, 3943. (c) Williams, R. V. *Chem. Rev.* **2001**, *101*, 1185–1204. (d) Dewar, M. J. S.; Jie, C. *Tetrahedron* **1988**, *44*, 1351–1358. (e) For a recent paper on hetero-substituted variants, see: Reiher, M.; Kirchner, B. *Angew. Chem., Int. Ed.* **2002**, *41*, 3429–3433.

- (3) Recent theoretical studies on barbaralanes and semibullvalenes include: (a) Wu, H.-S.; Jiao, H.; Wang, Z.-X.; Schleyer, P. v. R. *J. Am. Chem. Soc.* **2003**, *125*, 10524–10525. (b) Goren, A. C.; Hrovat, D. A.; Seefelder, M.; Quast, H.; Borden, W. T. *J. Am. Chem. Soc.* **2002**, *124*, 3469–3472. (c) Brown, E. C.; Henze, D. K.; Borden, W. T. *J. Am. Chem. Soc.* **2002**, *124*, 14977–14982, and references therein.
- (4) For leading references, see: (a) Williams, R. V. *Eur. J. Org. Chem.* **2001**, 227–235. (b) Jiao, H.; Nagelkerke, R.; Kurtz, H. A.; Williams, R. V.; Borden, W. T.; Schleyer, P. v. R. *J. Am. Chem. Soc.* **1997**, *119*, 5921–5929. (c) See also ref 2c.
- (5) (a) Tantillo, D. J.; Hoffmann, R. *Angew. Chem., Int. Ed.* **2002**, *41*, 1033–1036. (b) Tantillo, D. J.; Hoffmann, R. *J. Am. Chem. Soc.* **2002**, *124*, 6836–6837. (c) Tantillo, D. J.; Hoffmann, R. *Helv. Chim. Acta.* **2003**, *86*, 3525–3532. (d) Tantillo, D. J.; Hoffmann, R. *Eur. J. Org. Chem.* **2004**, 273–280.

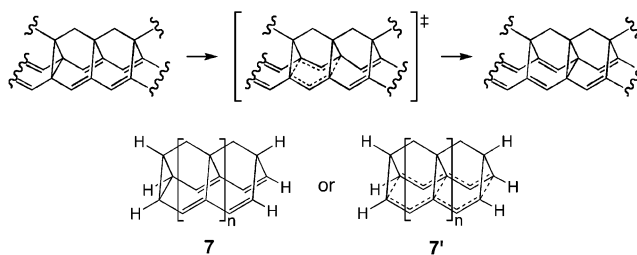
Methods

All density functional calculations were performed with *GAUSSIAN98*.⁶ Geometries were optimized (without symmetry constraints) at the B3LYP/6-31G(d) level,⁷ whose effectiveness in describing structures and energetics for pericyclic reactions, including [3,3]-sigmatropic shifts, is well documented.^{1d,8} In particular, the B3LYP method has been applied successfully to the study of [3,3]-sigmatropic shifts in barbaralanes and related structures.³ The stabilities⁹ of restricted B3LYP wave functions (toward unrestricted alternatives) for various closed-shell structures were verified using the “stable” keyword in *GAUSSIAN98*⁶ or by reoptimizing RB3LYP structures using UB3LYP and the “guess = (mix,always)” option. In some cases, searches for singlet diradicals were also performed using optimized triplets as starting points. All structures were characterized by frequency calculations at the B3LYP/6-31G(d) level, and zero-point energy corrections (scaled by 0.9806)¹⁰ from these calculations are included in the reported energies. Singlet diradical structures all had $\langle S^2 \rangle$ values close to 1, and their relative energies reported herein have not been corrected in any way for state mixing. For some structures (see text), nucleus-independent chemical shift (NICS)¹¹ calculations were performed using the GIAO-B3LYP/6-31G(d) method, and magnetic susceptibility calculations were performed using the CSGT-B3LYP/6-311+G** method;¹² unless otherwise noted, geometries optimized at the B3LYP/6-31G(d) level were used. For several structures (see text), CASSCF and CASPT2 calculations were also performed using MOLCAS.¹³ Ball-and-stick structural drawings were produced using Ball & Stick (N. Müller and A. Falk, *Ball & Stick V.3.7.6*, molecular graphics application for MacOS computers, Johannes Kepler University Linz, 2000).

Results and Discussion

I. Fused Barbaralanes. To hold the two polyene chains in **5** together, we initially chose a linking framework that resembles barbaralane (Scheme 2, compare with **1**). Oligomeric models **7/7'** were used to study these systems.

Scheme 2



The computed barrier for the Cope rearrangement of **7** ($n = 0$; barbaralane, **1**) through a transition structure of C_{2v} symmetry (**7'**, $n = 0$) is 6.6 kcal/mol (Figure 1).¹⁴ Somewhat surprisingly, no analogous transition structures for any of the other structures **7** studied ($n = 1, 2, 3$) could be located. Instead, optimizations produced singlet C_{2v} structures (**7'**, $n = 1, 2, 3$) that were shown by frequency calculations to be minima (Figure 1). Despite being optimized using restricted B3LYP calculations, the geometries of these structures consistently resembled pairs of polyenyl radicals held in close proximity. For example, the carbon–carbon bond lengths in each polyene chain of **7'** ($n = 2$) are 1.36, 1.43, 1.40, 1.40, 1.43, and 1.36 Å, while those of a simple extended heptatrienyl radical computed with UB3LYP/6-31G(d) are 1.36, 1.43, 1.39, 1.39, 1.43, and 1.36 Å. In addition, the RB3LYP wave functions for all of these structures were found to be stable toward unrestricted alternatives.¹⁵ The fact that such singlet-coupled bis-polyenyl radical structures were produced with restricted B3LYP calculations indicates that there must be significant interaction between the radical chains. This appears to be a through-space interaction, as shown in Figure 2.¹⁶

UB3LYP optimized triplet species have geometries similar to **7'** ($n = 0-3$) but with increased inter-polyene distances (Figure 1), since for this spin state the favorable inter-polyene orbital interaction is ineffectual. Since this is a through-space interaction between orbitals with nodes close to the nonbridgehead carbons, one would also expect the carbon–carbon bond lengths within the polyenes to be relatively insensitive to multiplicity; this is, in fact, what is observed (Figure 1).

That we compute a significant singlet–triplet gap, favoring the singlet configuration, for each of these structures (Figure 1) again argues for stabilizing interactions in the C_{2v} singlets.^{3c} In effect, by fusing two or more barbaralanes together, fully delocalized C_{2v} structures become minima rather than transition structures. This is consistent with the fact that conjugating substituents located on the alkene termini of barbaralane (**1**) and semibullvalene (**2**) lower the [3,3]-shift barrier.^{2,4}

- (6) Frisch, M. J.; Trucks, G. W.; Schlegel, H. B.; Scuseria, G. E.; Robb, M. A.; Cheeseman, J. R.; Zakrzewski, V. G.; Montgomery, J. A., Jr.; Stratmann, R. E.; Burant, J. C.; Dapprich, S.; Millam, J. M.; Daniels, A. D.; Kudin, K. N.; Strain, M. C.; Farkas, O.; Tomasi, J.; Barone, V.; Cossi, M.; Cammi, R.; Mennucci, B.; Pomelli, C.; Adamo, C.; Clifford, S.; Ochterski, J.; Petersson, G. A.; Ayala, P. Y.; Cui, Q.; Morokuma, K.; Malick, D. K.; Rabuck, A. D.; Raghavachari, K.; Foresman, J. B.; Cioslowski, J.; Ortiz, J. V.; Stefanov, B. B.; Liu, G.; Liashenko, A.; Piskorz, P.; Komaromi, I. R.; Gomperts, R.; Martin, L.; Fox, D. J.; Keith, T.; Al-Laham, M. A.; Peng, C. Y.; Nanayakkara, A.; Gonzalez, C.; Challacombe, M. P.; Gill, M. W.; Johnson, B.; Chen, W.; Wong, M. W.; Andres, J. L.; Gonzalez, C.; Head-Gordon, M.; Replogle, E. S.; Pople, J. A. *GAUSSIAN98*, revision A.9; Gaussian, Inc.: Pittsburgh, PA, 1998.
- (7) (a) Becke, A. D. *J. Chem. Phys.* **1993**, *98*, 5648–5652. (b) Becke, A. D. *J. Chem. Phys.* **1993**, *98*, 1372–1377. (c) Lee, C.; Yang, W.; Parr, R. G. *Phys. Rev. B* **1988**, *37*, 785–789. (d) Stephens, P. J.; Devlin, F. J.; Chabalowski, C. F.; Frisch, M. J. *J. Phys. Chem.* **1994**, *98*, 11623–11627.
- (8) (a) Wiest, O.; Montiel, D. C.; Houk, K. N. *J. Phys. Chem. A* **1997**, *101*, 8378–8388. (b) Houk, K. N.; Beno, B. R.; Nendel, M.; Black, K.; Yoo, H. Y.; Wilsey, S.; Lee, J. K. *J. Mol. Struct. (THEOCHEM)* **1997**, *398*, 399–169–179. (c) Hrovat, D. A.; Beno, B. R.; Lange, H.; Yoo, H.-Y.; Houk, K. N.; Borden, W. T. *J. Am. Chem. Soc.* **2000**, *122*, 7456–7460. (d) Guner, V.; Khuong, K. S.; Leach, A. G.; Lee, P. S.; Bartberger, M. D.; Houk, K. N. *J. Phys. Chem. A* **2003**, *107*, 11445–11459.
- (9) (a) Goldstein, E.; Beno, B.; Houk, K. N. *J. Am. Chem. Soc.* **1996**, *118*, 6036–6043. (b) Gräfenstein, J.; Cremer, D. *Mol. Phys.* **2001**, *99*, 981–989. (c) Yamanaka, S.; Kawakami, T.; Nagao, H.; Yamaguchi, K. *Chem. Phys. Lett.* **1994**, *231*, 25–33. (d) Yamaguchi, K.; Jensen, F.; Dorigo, A.; Houk, K. N. *Chem. Phys. Lett.* **1988**, *149*, 537–542. (e) Bauemschmitt, R.; Ahlrichs, R. *J. Chem. Phys.* **1996**, *104*, 9047–9052. (f) Beno, B. R.; Fennen, J.; Houk, K. N.; Linder, H. J.; Hafner, K. *J. Am. Chem. Soc.* **1998**, *120*, 10490–10493. (g) Staroverov, V. N.; Davidson, E. R. *J. Am. Chem. Soc.* **2000**, *122*, 186–187.
- (10) Scott, A. P.; Radom, L. *J. Phys. Chem.* **1996**, *100*, 16502–16513.
- (11) (a) Schleyer, P. v. R.; Maerker, C.; Dransfeld, A.; Jiao, H. J.; Hommes, N. J. R. v. E. *J. Am. Chem. Soc.* **1996**, *118*, 6317–6318. (b) Schleyer, P. v. R.; Manoharan, M.; Wang, Z.-X.; Kiran, B.; Jiao, H.; Puchta, R.; Hommes, N. J. R. v. E. *Org. Lett.* **2001**, *3*, 2465–2468.
- (12) (a) Jiao, H. J.; Schleyer, P. v. R. *Angew. Chem., Int. Ed. Engl.* **1995**, *34*, 334–337. (b) Jiao, H. J.; Schleyer, P. v. R. *J. Phys. Org. Chem.* **1998**, *11*, 655–662. (c) The CSGT method: Keith, T. A.; Bader, R. W. F. *Chem. Phys. Lett.* **1993**, *210*, 223–231.

- (13) (a) Andersson, K.; Malmqvist, P.-Å.; Roos, B. O.; Sadlej, A. J.; Wolinski, K. *J. Phys. Chem.* **1990**, *94*, 5483–5488. (b) Andersson, K.; Malmqvist, P.-Å.; Roos, B. O. *J. Chem. Phys.* **1992**, *96*, 1218–1226. (c) Borden, W. T.; Davidson, E. R. *Acc. Chem. Res.* **1996**, *29*, 67–75, and references therein. (d) Andersson, K.; Blomberg, M. R. A.; Fülcher, M. P.; Karlström, G.; Lindh, R.; Malmqvist, P.-Å.; Neogrády, P.; Olsen, J.; Roos, B. O.; Sadlej, A. J.; Schütz, M.; Seijo, L.; Serrano-Andrés, L.; Siegbahn, P. E. M.; Widmark, P.-O. *MOLCAS, version 5.0*; Department of Theoretical Chemistry, Chemical Centre: University of Lund, P.O.B. 124, S-221 00 Lund, Sweden, 1997.
- (14) This value was also calculated at the same level in ref 3a.
- (15) **7'** ($n = 1$) was also optimized with both MP2/6-31G(d) and CASSCF(10,10)/6-31G(d). In both cases, delocalized structures resulted that are extremely similar to that found with B3LYP/6-31G(d) (see Figure 1).
- (16) For two similarly tethered infinite polyacetylene chains, a second set of orbitals is also present, with coefficients on the other carbons of the polyene chains. The nature of the linking framework would keep these carbons quite a bit farther apart than the bridgehead carbons, however, leading to only very small through-space interactions and a pair of nearly degenerate orbitals at the orbital frontier. It is possible, therefore, that the infinite system might have a triplet ground state, albeit of a rather different nature than the oligomers we study.

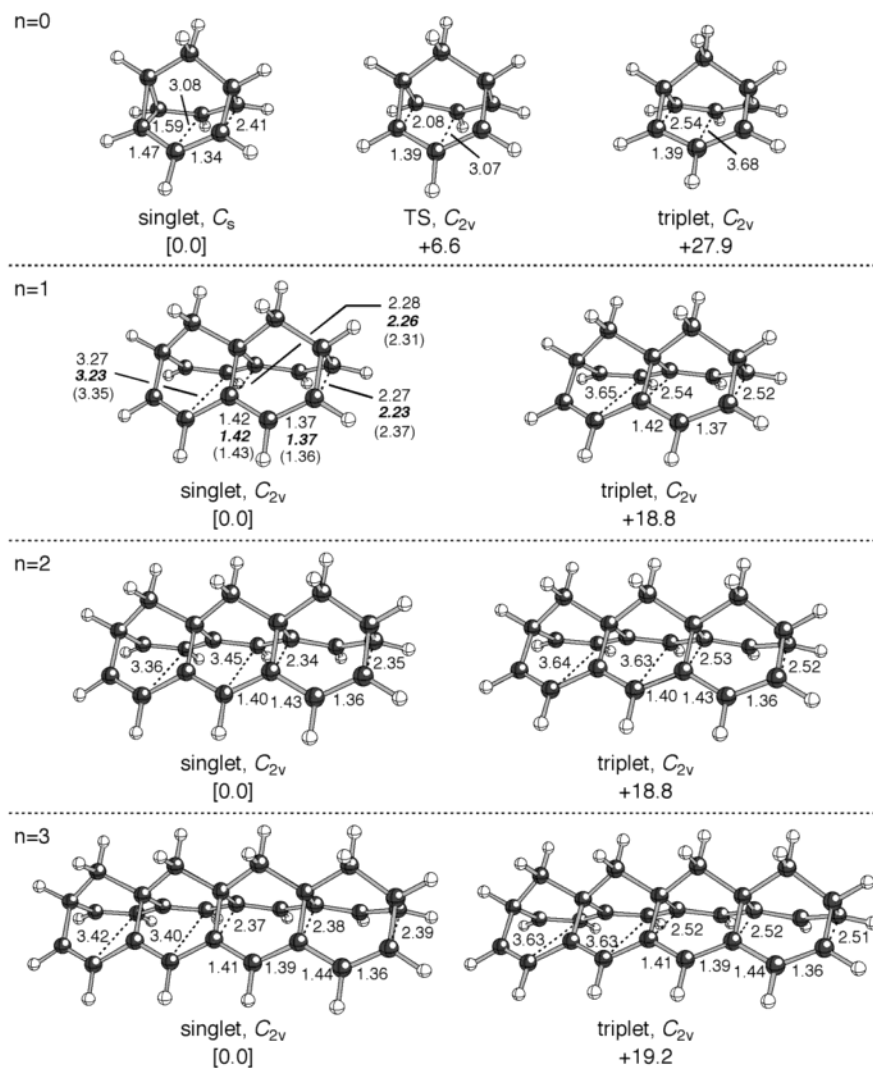


Figure 1. Optimized singlet and triplet structures ($7'7'$, $n = 0-3$). All structures are minima at the B3LYP/6-31G(d) level, except the [3,3] transition structure (TS) shown for $n = 0$. Relative energies of singlets and triplets for each value of n are shown in kcal/mol. Selected distances are shown in Å. B3LYP/6-31G(d) optimized distances are in normal text, CASSCF(10,10)/6-31G(d) optimized distances (for $n = 1$) are in parentheses, and MP2/6-31G(d) optimized distances (for $n = 1$) are in bold italics.

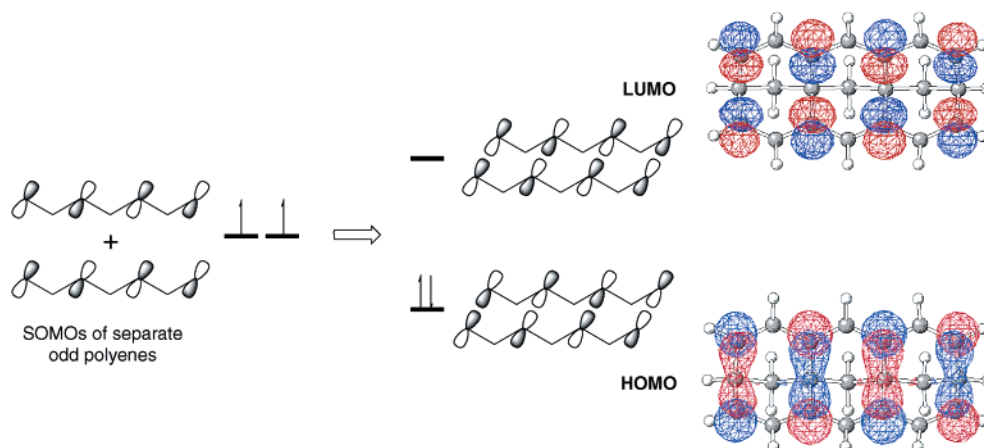


Figure 2. Combination of individual polyenyl SOMOs to produce the HOMO and LUMO of delocalized singlet $7'$ ($n = 2$). Actual orbitals from a B3LYP/6-31G(d) calculation are shown at right, viewed from “below” the molecule (i.e., from the face opposite the linking backbone).¹⁶

Computed magnetic susceptibilities also indicate that $7'$ ($n = 0-3$) are aromatic. Table 1 shows these values for $7'$ ($n = 0-3$) and their corresponding triplets (see Figure 1). Magnetic susceptibilities are considerably and consistently more negative

for the singlets compared to the triplets. In addition, computed values for structures with localized interpolyene bonds (see section III below) were intermediate between those of the singlets and triplets, indicating that the susceptibilities of $7'$ (n

Table 1. Magnetic Susceptibilities (χ , CSGT-B3LYP/6-311+G**, cgs-ppm) for Singlet and Triplet Structures (**7'**, $n = 0-3$) Shown in Figure 1

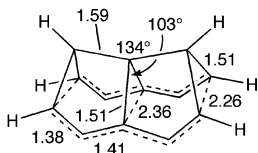
n	singlet or triplet	χ
0	S	-90.2
	T	-59.1
1	S	-145.8
	T	-94.5
2	S	-202.6
	T	-124.7
3	S	-261.2
	T	-149.9

$n = 0-3$) are indeed enhanced through transannular delocalization. These data are consistent with aromaticity in the singlets and some degree of antiaromaticity in the triplets.¹² Thus, structures **7'** ($n = 1-3$) appear to be 10π , 14π , and 18π bis-homoaromatic species!

We have thus come (theoretically) to a new class of delocalized molecules in which two polyenyl radical chains interact with each other through space in a bonding way, but do not form full σ -bonds. Let us try some variations on the theme and then seek a relationship to another, well-known class of molecules.

II. Trying Different Linkers. Several other frameworks for holding together two polyenes were also explored. First, consider the model systems (**8-12**) shown in Table 2. For each of the different linkers considered, delocalized bis-polyenyl radical-like structures were found to be minima. In structure **8**, the polybarbaralane framework has been broken into separate barbaralane units connected through the polyene chains rather than through the linkers as in **7/7'**. In **8**, there is, of course, severe steric congestion between the hydrogens of neighboring barbaralane units (the $H\cdots H$ distance in **8** is 1.7 Å), and an overall curved structure of the molecule that minimizes this repulsion is computed. Despite the obvious strain in this molecule, short inter-polyene contacts are still observed for all of the bridgehead carbons and no distortion toward localized barbaralane units is apparent. A similar situation is found for **9**, where we tried isolated semibullvalene units, rather than barbaralane units. Again, central steric congestion is observed, although it is less severe than for **8** (the central $H\cdots H$ distance in **9** is 2.2 Å) and does not induce the molecule to curve.¹⁷ For both **8** and **9**, singlets with interacting polyenyl groups are considerably more stable and have much more negative magnetic susceptibilities than corresponding triplets (Table 2).

(17) One system with fused semibullvalene units was also examined (selected distances shown in Å):



This molecule is a highly strained (note in particular the 134° angle at the central carbon) and curved molecule (now with a direction of curvature opposite that of **8**), but still contains close interpolyene contacts. This molecule can also be considered a member of the class of molecules known as fenestranes: molecules containing a central quaternary carbon that serves as a corner for four fused rings that are arrayed like the panes of a window or the "four corners" states of the American southwest. For leading references on fenestranes, see: (a) Georgian, V.; Saltzman, M. *Tetrahedron Lett.* **1972**, 4315-4317. (b) Thommen, M.; Keese, R. *Synlett* **1997**, 231, and references therein. It should be noted that a structure with a localized inter-polyene single bond at one end is slightly more stable than this structure (by ~ 2 kcal/mol, based on electronic energies).

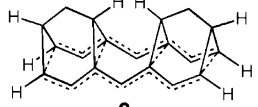
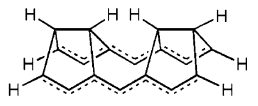
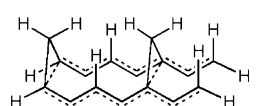
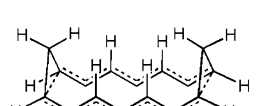
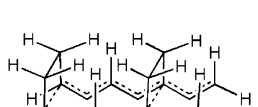
Further simplification of the bridging system in **7/7'** was also explored. In structures **10** and **11**, the two polyene chains are held together only by methylene bridges at various distances from each other. In both structures, the inter-polyene distances between the remaining bridgehead carbons are still short, but the distances between carbons that were bridgeheads in **7'**, **8**, and **9** (but no longer play that role in **10** and **11**) are considerably longer (Table 2). This is perhaps due to the steric congestion that arises when the bridges are replaced by hydrogens, which should discourage the inner polyene positions from being too close: $H\cdots H$ distances between these hydrogens, their counterparts on the other polyene, and those of the bridging methylenes range from 1.9 to 2.3 Å. Still, singlet structures are more stable than triplets and have much more negative magnetic susceptibilities (Table 2).

In structure **12**, the methylene bridges of **10** are replaced by ethylene bridges. This leads to significant changes to some inter-polyene distances, compared to those in **10**, especially in distances between bridgehead carbons (Table 1). Unlike structures **7'** and **8-11**, whose RB3LYP wave functions were found to be stable toward unrestricted alternatives, **12**'s wave function was found to be unstable. Reoptimization with UB3LYP led to a singlet diradical ($\langle S^2 \rangle = 1.03$) with all inter-polyene distances greater than 3 Å and that was approximately 5 kcal/mol more stable than the restricted structure (without spin-projection). Moreover, a triplet resembling the singlet diradical (but with slightly longer inter-polyene distances) and having approximately the same energy (0.8 kcal/mol above the singlet diradical without spin-projection) was also found. This is consistent with the fact that singlet-triplet gaps in semibullvalenes decrease as their polyenyl fragments interact less.^{3c} In addition to the small singlet-triplet gap, the similarity in magnetic susceptibilities for singlet and triplet **12** indicates that these structures contain essentially noninteracting polyenyl chains. The instabilities in this system may be connected with the steric problems imposed by the ethylene bridges (a slight skewing of the molecule occurs, which relieves eclipsing interactions in the ethylene bridges) and/or through-bond coupling between the polyenes and ethylene groups, which should reduce the HOMO/LUMO gap.

Several other variations were also explored. These (structures **13-23**) are shown in Table 3. In **7/7'**, the bridges holding the two polyenyl chains together are attached to the polyenes at their odd positions (i.e., at carbons 1, 3, 5, ... of each). In structures **13-17** (Table 3, left), however, the bridges are connected at even positions: the positions at which interpolyene orbital overlap is minimal (see Figure 2). Consequently, diradical species are found for singlets as well as triplets. Also, the inter-polyene distances in these species are greater than those in singlets **7'** and **8-11** (a typical geometry—that of singlet **16**—is shown in Figure 3; compare with Figure 1 and Table 2). Singlet-triplet gaps are also small, and χ 's for singlets and triplets are nearly equal.

Structures **18-23** (Table 3, right) have their linkers attached again at all of the odd positions of the two polyenyl groups, but now only methylene groups link the chains, and $H\cdots H$ repulsions between methylenes induce molecular curvature (as in **8**).¹⁸ In this collection of structures, some polyene bonds were allowed to assume *s-cis* rather than *s-trans* conformations with respect to the rest of their polyenyl chain, and in some cases

Table 2. Properties of 8–12^d

structure	symmetry after optimization	polyene bond lengths ^a (Å) in singlet	inter-polyene distances ^a (Å) in singlet	E_T-E_S	χ_S	χ_T
 8	C_{2v}	1.36 1.44 1.40	2.37 3.39 2.34 3.28	16.5	-190.9	-117.7
 9	C_{2v}	1.36 1.43 1.39	2.39 3.59 2.42 3.35	4.6	-169.1	-110.7
 10	C_s	1.37 1.42 1.40 1.39 1.45 1.35	2.30 3.41 2.76 3.37 2.36 3.51 3.27	7.2	-162.3	-102.7
 11	C_{2v}	1.37 1.42 1.39	2.28 3.53 3.13 3.91	4.6	-192.0	-100.0
 12	C_1	1.36 ^b 1.43 1.39 1.40 1.44 1.36	2.82 3.38 2.80 3.27 2.69 3.37 3.12	0.8 ^c	-136.3 ^c	-131.4

^a Distances in order starting from the left of each structure as drawn. ^b For this structure, only bond lengths from one of the polyene chains are shown; those from the other are all within 0.01 Å of their counterparts. ^c For unrestricted **12**. ^d Distances are for singlets optimized with restricted B3LYP/6-31G(d). Singlet–triplet gaps (E_T-E_S) are in kcal/mol, and magnetic susceptibilities (χ , CSGT-B3LYP/6-311+G***) are in cgs-ppm

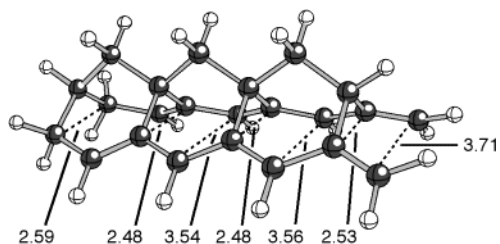
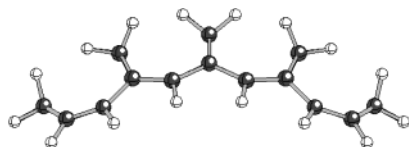


Figure 3. Optimized geometry of singlet **16**. Selected distances are shown in Å.

terminal methylene linkers were initially placed on the face of the molecule opposite the internal linkers (**19**, **21**, **22**). These structural changes have dramatic effects on the nature of the bis-polyenyl species. First and foremost, interpolyene delocalization appears not to extend through the *s-cis* portions of these structures: the terminal alkenes are nearly orthogonal to the rest of the polyenyl chains (a typical geometry of this type is shown in Figure 4). Comparing **18** to **19** and **20** to **21** to **22**, one can see that conjugation of each additional 4π electron unit (in the form of two suitably oriented alkenes, one from each

(18) A “side view” of structure **23**:

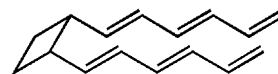


polyenyl chain) to a preexisting delocalized bis-polyenyl unit is worth approximately 10–13 kcal/mol.

Overall, the series of structures shown in Tables 2 and 3 demonstrate that the inter-polyene interactions are quite sensitive to the nature of the linkers that hold the two polyenyl chains together.^{19,20} Thus, a rigid framework is essential for promoting efficient inter-polyene interactions.

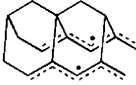
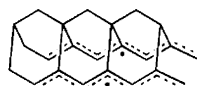
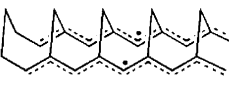
III. Localized Alternatives. For cases with clear inter-polyene delocalization—**7/7'**, **8–11**, **18**, **20**, and **23**—additional calculations were performed in order to check whether the fully delocalized structures were lower in energy than structures with localized alkenes and inter-polyene single bonds (Chart 1). Several strategies were used to find localized structures, including (1) constrained B3LYP/6-31G(d) optimizations (with one inner or terminal inter-polyene distance fixed at 1.60 Å), followed by full optimizations; (2) B3LYP/STO-3G optimizations using AM1 starting structures, followed by B3LYP/6-31G-

(19) We have not yet studied the seemingly less constrained way to hold two polyenes in proximity to each other that has been explored by W. von E. Doering and co-workers and Hopf and co-workers (Doering, W. von E.; He, J.; Shao, L. *J. Am. Chem. Soc.* **2001**, *123*, 9153–9151; Schüll, V.; Hopf, H. *Tetrahedron Lett.* **1981**, *22*, 3439–3442), who examined derivatives of bis-polyenyl cyclobutanes:



(20) σ -Bond cleavage in certain polyenes to produce two polyenyl radicals has been shown previously to be facile. See, for example: Beno, B. R.; Fennen, J.; Houk, K. N.; Lindner, H. J.; Hafner, K. *J. Am. Chem. Soc.* **1998**, *120*, 10490–10493, and ref 19.

Table 3. Properties of Structures 13–23^d

structure	$E_{\text{rel(S)}}$	$E_{\text{rel(T)}}$	χ_{S}	χ_{T}	structure	$E_{\text{rel(S)}}$	$E_{\text{rel(T)}}$	χ_{S}	χ_{T}
	0.0	0.9	-84.8	-82.6		0.0	8.5	-124.0	-85.4
	0.0	1.0	-125.0	-120.6		13.0 ^a	b	-112.5	b
	0.0	0.8	-91.4	-88.6		0.0	8.9	-164.4	-114.5
	0.0	1.2	-164.0	-156.9		10.0 ^c	19.3 ^c	-158.8	-116.2
	0.0	0.7	-165.6	-162.1		23.2 ^c	31.2 ^c	-147.7	-117.6
						0.0	9.8	-206.9	-117.6

^a Relative to singlet **18**. ^b Attempts to optimize the triplet form of **19** led to the triplet form of **18**. ^c Relative to singlet **20**. ^d Geometries of both singlets (S) and triplets (T) were optimized with B3LYP/6-31G(d). Magnetic susceptibilities (χ) were calculated for these geometries using CSGT-UB3LYP/6-311+G**. Relative energies are in kcal/mol, and magnetic susceptibilities are in cgs-ppm

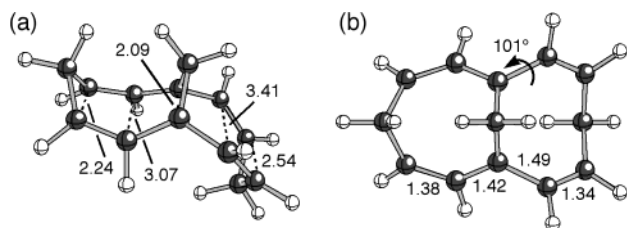
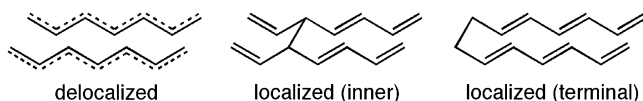


Figure 4. Optimized geometry of singlet **19**. Selected distances are shown in Å. (a) Side view. (b) Top view.

Chart 1



(d) single points and/or full optimizations; and (3) full B3LYP/6-31G(d) optimizations using AM1 starting structures.

Let us first consider some structures with “inner” interpolyene single bonds. For **7/7'** ($n = 1$), a minimum with an internal single bond (1.69 Å) could be located only at the B3LYP/STO-3G level. This structure is, based on purely electronic energies, 15.4 kcal/mol above that for delocalized **7'** ($n = 1$). For **7/7'** ($n = 2$), **8**, **9**, and **10**, B3LYP/6-31G(d) optimizations with one inner bond fixed at 1.60 Å, followed by full optimizations, led back to fully delocalized structures. For **7'** ($n = 2$), **8**, and **9**,

Table 4. Properties of Localized (end-closed) Stationary Points^f

structure	terminal inter-polyene distance (Å)	relative energy (kcal/mol) ^a	χ (cgs-ppm) ^b
7 ($n = 0$)	1.61	-6.6 (-5.2)	-80.0
7 ($n = 1$)	1.64	0.8 (4.4)	-127.8
7 ($n = 2$)	1.67	5.6 (11.5)	-179.6
7 ($n = 3$)	1.61 ^c	<i>d</i> (16.9)	-216.2
8 (localized)	1.69	6.3	<i>e</i>
9 (localized)	1.656	6.5	<i>e</i>
18 (localized)	1.60	-0.4	-102.7
20 (localized)	1.54	6.2	-139.7
23 (localized)	1.64	10.6	-177.8

^a No parentheses: B3LYP/6-31G(d); in parentheses: B3LYP/6-31G(d)//B3LYP/STO-3G. ^b Computed at the CSGT-UB3LYP/6-311+G** level. ^c From the geometry computed at the B3LYP/STO-3G level. ^d Not a stationary point at the B3LYP/6-31G(d) level. ^e Not computed. ^f Energies are relative to those of corresponding fully delocalized structures.

the constrained structures were approximately 20 kcal/mol higher in energy than the fully delocalized structures. For **10**, the constrained structure was 11 kcal/mol less stable than the delocalized structure. For structure **11**, a minimum with a localized internal single bond (1.58 Å) was found using B3LYP/6-31G(d), presumably because of the increased flexibility of this structure compared to the others (structure **11** only has interpolyene bridges at its ends). Still, this localized structure is approximately 4 kcal/mol higher in energy than the delocalized

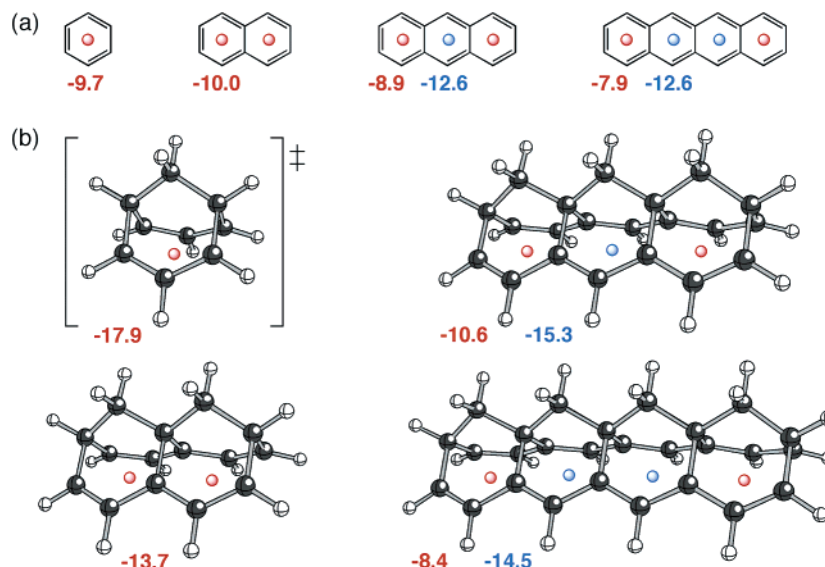


Figure 5. NICS values computed at the GIAO-B3LYP/6-31G(d) level for the points represented by small spheres.

Table 5. Relative Energies of Fully Delocalized $7'$ ($n = 1$) and Localized (end-closed) Alternative Structures at Various Levels of Theory

structure	relative energy (kcal/mol vs open)				
	B3LYP/6-31G(d)// B3LYP/6-31G(d)	CASSCF(10,10)/6-31G(d)// B3LYP/6-31G(d)	CASPT2/6-31G(d)// B3LYP/6-31G(d)	CASSCF(10,10)/6-31G(d)// CASSCF(10,10)/6-31G(d)	CASPT2/6-31G(d)// CASSCF(10,10)/ 6-31G(d)
open	0.0	0.0	0.0	0.0	0.0
end-closed	0.2	-5.9	0.2	-5.4	-0.6

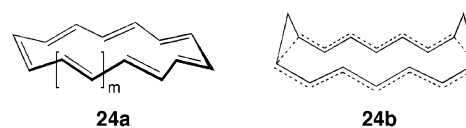
structure. It seems, therefore, that formation of “inner” interpolyene single bonds is not favorable.

Is the same true for formation of terminal single bonds? The data in Table 4 show that end-closed structures are comparable in energy (albeit for different reasons, as shown by the magnetic susceptibilities) to fully delocalized structures for $7/7'$ ($n = 1$) and **18**, but the more extensively conjugated delocalized structures ($7'$ ($n = 2, n = 3$), **8**, **9**, **20**, and **23**) are clearly more stable than their localized counterparts.²¹ The data appear to indicate a diminishing additive effect of extending the conjugation, but this point will require further investigation. For **10** and **11**, localized minima with terminal bond lengths of 1.63 and 1.60 Å, respectively, were also found, but these two minima were actually 0.3 and 3.3 kcal/mol lower in energy than the corresponding fully delocalized structures, despite the fact that their polyenyl fragments are the same length as those in $7'$ ($n = 2$), **8**, **9**, and **20**. In **10** and **11**, localization of the inter-polyene interactions at one end apparently allows for relief of transannular strain in the remainder of the molecule. Although the RB3LYP wave functions for all of the localized minima were found to be stable toward unrestricted alternatives, higher level (multiconfigurational) calculations may ultimately be required to pin down the relative energies of localized and delocalized structures in cases where we have computed that they are close in energy.^{21–23} Nonetheless, it appears that structures with interpolyene delocalization are generally more stable than alternative structures with inner or terminal interpolyene single bonds.

(21) CASSCF(14,14)/6-31G(d) and CASPT2/6-31G(d) single-point calculations agree that the fully delocalized $7'$ ($n = 2$) is more stable than the end-closed form (by ~ 1 kcal/mol with CASSCF and by ~ 6 kcal/mol with CASPT2).

(22) B3LYP was also previously shown to give energy differences for **7** and $7'$ ($n = 0$, barbaralane) that were quite similar to those computed with CASPT2. See ref 3c.

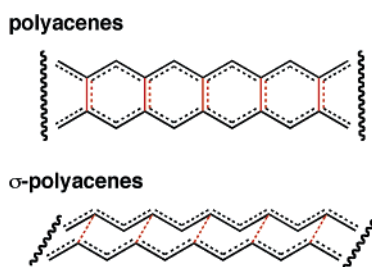
IV. Analogies. How should we view structures such as $7'$ and the closely related **8–11**, **18**, **20**, and **23**? They share characteristics with several classes of organic molecules. First, they resemble homoconjugated trannulenes. Trannulenes are cyclic conjugated polyenes containing only *trans* double bonds (**24a**).²⁴ The π -orbitals in these zigzagging polyene rings are radially disposed. Similarly, structures such as $7'$ ($n = 1, 2, 3$), **8–11**, **18**, **20**, and **23** also contain zigzagging polyene chains, but here connected into loops by saturated bridges (**24b**). There are clearly interactions across these bridges, producing homoconjugated analogues of the π -cycles in normal trannulenes. This analogy breaks down, however, when we consider that additional transannular interactions across the “interior” of most of these structures are of comparable strength to those across their terminal bridges.



Structures $7'$ ($n = 1–3$) can also be thought of as arising from the fusion of several copies of the transition structure for

(23) Structures for $7'$ ($n = 1$) with localized terminal inter-polyene bonds were also explored using the B3LYP/6-31G(d)//B3LYP/6-31G(d), CASSCF(10,10)/6-31G(d)//B3LYP/6-31G(d), CASPT2/6-31G(d)//B3LYP/6-31G(d), CASSCF(10,10)/6-31G(d)//CASSCF(10,10)/6-31G(d), and CASPT2/6-31G(d)//CASSCF(10,10)/6-31G(d) levels. The results are shown in Table 5. B3LYP and CASPT2 energy calculations agree that the end-closed and open (fully delocalized) structures are very similar in energy—irrespective of the method used for the geometry optimization—while CASSCF consistently predicts that the end-closed form is considerably more stable than the open form (by 5–6 kcal/mol). Generally, CASPT2 energy calculations are considered to be more reliable than CASSCF energy calculations, and B3LYP has been shown to give similar results to CASPT2 for various reactions.^{8d,22}

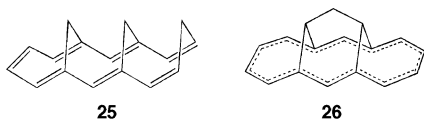
Chart 2



the [3,3]-sigmatropic shift in barbaralane ($7'$, $n = 0$). Various barbaralane analogues and derivatives have been examined previously in pursuit of “stable transition states”: systems for which the delocalized structure is actually a minimum on the potential energy surface.² In the case of structures $7'$ ($n = 1-3$), the barbaralane subunits are all certainly delocalized in the minima. But there is not one transition state (for six carbons, or for all the polyene carbons) that is being stabilized. Instead, it is more like a whole family of barbaralane transition states collapsed into a single minimum.²⁵

There is a more interesting relationship to focus on for $7'$ ($n = 1-3$), **8-11**, **18**, **20**, and **23**. These structures share several important characteristics with the polyacenes (**6**).²⁶ Both types of systems can be thought of as being comprised of two polyene chains held in close proximity by an organic framework and interacting with each other. In the case of the normal polyacenes (**6**), the π -orbitals of the polyene chains interact with each other in a π -sense, while in molecules such as $7'$ ($n = 1-3$), **8-11**, **18**, **20**, and **23**, the π -orbitals of the polyene chains interact with each other in a σ -sense (Figure 2). Because of the similarity of these orbital interactions, we think that structures such as $7'$ are best characterized as “ σ -polyacenes” (Chart 2).

Intermediate between the polyacene and σ -polyacene extremes are hybrid structures such as the known “hairpin polyenes” (e.g., **25**)²⁷ and bridged annulenes (e.g., **26**).²⁸



- (24) (a) Fokin, A. A.; Jiao, H.; Schleyer, P. v. R. *J. Am. Chem. Soc.* **1998**, *120*, 9364–9365. (b) Wei, X.-W.; Darwish, A. D.; Boltalina, O. V.; Hitchcock, P. B.; Street, J. M.; Taylor, R. *Angew. Chem., Int. Ed.* **2001**, *40*, 2989–2992. (c) Havenith, R. W. A.; Rassat, A.; Fowler, P. W. *J. Chem. Soc., Perkin Trans. 2* **2002**, 723–727. (d) Darwish, A. D.; Kuvytchko, I. V.; Wei, X. W.; Boltalina, O. V.; Gol'dt, I. V.; Street, J. M.; Taylor, R. *J. Chem. Soc., Perkin Trans. 2* **2002**, 1118–1121.
- (25) There is a relationship between this collective “transition state” and the geometry of a hypothetical (still) metallic allotrope of carbon. See: Hoffmann, R.; Hughbanks, T.; Kertesz, M.; Bird, P. H. *J. Am. Chem. Soc.* **1983**, *105*, 4831–4832.
- (26) (a) Wiberg, K. B. *J. Org. Chem.* **1997**, *62*, 5720–5727. (b) Houk, K. N.; Lee, P. S.; Nendel, M. *J. Org. Chem.* **2001**, *66*, 5517–5521, and references therein.

Are characteristic properties of normal polyacenes also displayed by the σ -polyacenes? The aromaticity of individual rings in several polyacenes has been probed previously using nucleus-independent chemical shift (NICS) calculations.^{11,29} NICS values at the center of each ring of the four smallest polyacenes (benzene, naphthalene, anthracene, and tetracene) are shown in Figure 5a.³⁰ The NICS values of the terminal rings in these systems decrease in magnitude as they become longer, and inner rings have larger NICS values than the terminal rings. A similar trend is observed for the NICS values of the σ -polyacenes $7'$ ($n = 0-3$) (computed at the centroids of each set of six polyene carbons corresponding to one barbaralane unit, Figure 5b). For comparison, the computed NICS value for the triplet corresponding to $7'$ ($n = 1$) is +3.6, again showing that the polyene orbitals interact effectively only in the singlet. These results are entirely consistent with those from our magnetic susceptibility calculations as well.

Conclusions

We have described a new class of theoretical molecules—the σ -polyacenes—that are characterized by through-space interactions between polyenyl groups and significant bis-homoaromaticity. While the polyacene/ σ -polyacene analogy is not perfect, its core—that both boast interacting polyene chains—still provides a useful framework for understanding their structures. Given the interest in the electronic properties of polyacenes,²⁶ we think that σ -polyacenes are also attractive targets for synthesis.

Acknowledgment. We gratefully acknowledge support from the National Science Foundation (CHE0204841, CHE9909893, CHE9808182) and the National Computational Science Alliance. D.K.H. thanks the Mary M. Gates foundation for generous support. We are grateful to Professor Wes Borden for facilitating the calculations performed at the University of Washington.

Supporting Information Available: Coordinates and energies for structures in Figure 1 and Tables 2 and 3, along with an expanded discussion of singlet/triplet and HOMO/LUMO gaps. This material is available free of charge via the Internet at <http://pubs.acs.org>.

JA0392364

- (27) Frölich, W.; Dewey, H. J.; Deger, H.; Dick, B.; Klingensmith, K. A.; Püttmann, W.; Vogel, E.; Hohlneicher, G.; Michl, J. *J. Am. Chem. Soc.* **1983**, *105*, 6211–6220. The presence of “weak transannular interactions” has been suggested for these molecules.
- (28) (a) Vogel, E.; Brinker, U. H.; Nachtkamp, K.; Wassen, J.; Mullen, K. *Angew. Chem.* **1973**, *85*, 760–762. (b) Gunther, H.; Schmickler, H.; Brinker, U. H.; Nachtkamp, K.; Wassen, J.; Vogel, E. *Angew. Chem.* **1973**, *85*, 762–763, and references therein.
- (29) Application of the NICS technique to the polyacenes is described in: Schleyer, P. v. R.; Manoharan, M.; Jiao, H.; Stahl, F. *Org. Lett.* **2001**, *3*, 3643–3646. For a related study, see: Poater, J.; Fradera, X.; Duran, M.; Solà, M. *Chem. Eur. J.* **2003**, *9*, 1113–1122.
- (30) The NICS values in Figure 5 were computed at the GIAO-B3LYP/6-31G-(d) level. These are similar to (and consistently ~1 ppm more negative than) those computed previously at the IGLO/DZ2P/B3LYP/6-311+G** level: –9.7 for benzene, –8.9 for naphthalene, –7.6 and –11.5 for anthracene, and –6.6 and –11.4 for tetracene.²⁹